

# Residual Stress and Heat Treatment – Process Design for Bending Fatigue Strength Improvement of Carburized Aerospace Gears

B. Lynn Ferguson<sup>1</sup>, Andrew M. Freborg<sup>1</sup>, Zhichao Li<sup>1</sup>

<sup>1</sup>*Deformation Control Technology, Inc., 7261 Engle Road Suite 105, Cleveland, OH 44130, USA,  
Lynn.Ferguson@DeformationControl.com*

## Abstract

It is well established that carburization of low alloy steels promotes compressive residual surface stress upon quenching, and that compressive surface stresses enhance fatigue life. In an effort to build on these established facts, a project is in-progress to improve helicopter gear fatigue life the application of intensive quenching to achieve deeper compressive surface stress. Under US Army Sponsorship, DCT has demonstrated the feasibility of improving the bending fatigue life of Pyrowear 53 steel gears by achieving deeper compressive residual stress in carburized and quench hardened parts. Computer simulations of the conventional heat treatment practice and an intensive quenching process were conducted to analyze these heat treating processes in terms of metallurgical response and residual stress development. The timing and location of phase transformations during the quenching process was found to be critical to achieving the optimum residual stress state for service life. Beginning with simple notched bar coupons and progressing to full test gears, the physical bending fatigue results for these heat treated components are discussed in relation to the combined heat treatment residual and gear loading stresses from the computer simulations.

## Keywords

Computer simulation, residual stress, fatigue life, intensive quenching

## 1 Introduction

There is a need to increase the service life of helicopter transmission components while also increasing the power density of the transmission itself. This is similar to the need in the automotive industry to take weight out of the powertrain without degrading performance and life.

Under sponsorship of the Army Aviation Technology Directorate (AATD), a program was initiated to demonstrate the application of an innovative quenching process to achieve improved gear tooth bending fatigue strength. If successful, improved transmission performance could be achieved without an expensive redesign of the transmission components. The technology

applied in this effort was the use of intensive quenching in place of conventional immersion quenching in agitated oil to produce enhanced residual compressive surface stresses.

A prior program had demonstrated the feasibility of this approach for improving the fatigue life.[Freborg, 2005] Notched bars of Pyrowear 53 steel were carburized on one face and hardened conventionally or by intensive quenching, and then subjected to three point bending fatigue testing. The result was an improvement in bending strength for the intensively quenched samples, and this was related to greater surface compressive stress as measured by X-RAY diffraction and also predicted by computer simulation.

For this continuation effort, a spur gear was selected as the demonstration component, with single tooth bending fatigue tests to be performed at the Gear Research Laboratory associated with the Pennsylvania State University in State College, PA, USA. The gear has 40 teeth, a module of 2.54, and a face width of 6.35 mm (cf. Figure 1).



Figure 1: Spur gear used for bending fatigue test

## 2 Experimental Program

### 2.1 Pyrowear 53 Steel

Pyrowear 53 is a relatively high alloy, carburizing grade of steel (cf. Table 1) that has high hardenability and resistance to softening at temperature. These properties, plus an excellent combination of strength, toughness and fatigue resistance have resulted in this alloy being widely used as helicopter transmission gears. The high hardenability results in martensite being formed even in thick sections under slow cooling conditions. The martensite start temperature for the base carbon level is approximately 437° C and at a carbon level of 0.8 % by weight is 85° C.

<b>Fe</b>	<b>C</b>	<b>Mn</b>	<b>Si</b>	<b>Cr</b>	<b>Ni</b>	<b>Mo</b>	<b>Cu</b>	<b>V</b>
bal.	0.1	0.35	1.0	1.0	2.0	3.25	2.0	0.1

Table 1: Typical Alloy Chemistry of Pyrowear 53 Steel in Weight Percents.

### 2.2 Test Gear Manufacture

A total of thirty two Gears specifically designed for single tooth bend testing were purchased from Sikorsky Aircraft Corporation. The gears were machined from Pyrowear 53 bar stock in preparation for heat treatment (cf. Table 2). All 32 gears were vacuum carburized in one batch; prior to carburization, the gears were copper plated so that only the tooth flanks and root were carburized (cf. Figure 1). Sixteen gears were then hardened and tempered following the baseline schedule, and the remaining gears were hardened and tempered following the intensive quenching schedule (cf. Table 2). After tempering, approximately 0.13 mm of stock was ground from the tooth faces of the oil quenched gears, and 0.18 mm of stock was ground from the intensively quenched gears. The aim was for the only process difference to be the quench step,

so the effect of grind stock differences was investigated using simulation prior to proceeding with finish grinding.

	Carburize	Solution	Austenitize & Quench	1 <sup>st</sup> Temper	Cryogenic Treatment	2 <sup>nd</sup> Temper
BASELINE	8 Hours 927° C	Subcritical Anneal	Austenitize 913° C and Oil Quench	Temper at 450° F	Deep Freeze ≤ -80° C for 1 hour	Temper at 230° C
INNOVATION	8 Hours 927° C	Subcritical Anneal	Austenitize 913° C and Intensive Quench	Temper at 450° F	Deep Freeze ≤ -80° C for 1 hour	Temper at 230° C

Table 2: Heat Treat Schedules for the Two Sets of Gears.

### Differences in Growth During Hardening

The green dimensions of the gears were based on the conventional heat treat process (oil quenching), where, from experience, the growth after hardening provided a grind stock of 0.13 mm. The intensively quenched gears grew 0.05 mm more in the radial direction, thus requiring 0.18 mm of stock to be removed by grinding. This meant that more of the carburized case would be removed from the intensively quenched gears than from the oil quenched gears in order to meet final dimensions. While this magnitude seems small, it represents 5% of the aim 1.0 mm case depth. A concern was that this greater metal removal would this effectively wash-out any observable difference in residual stress state between the quench processes.

To investigate this possibility within the time constraint of a needed decision, heat treat simulation was used to predict the residual stress states and dimensional change for the two processes, and also to determine the reason for the difference. The simulations predicted that the radial displacements of the tooth tip and the root for the intensively quenched gear would be 0.051 to 0.064 mm greater than for the oil quenched gear. The carbon profile predicted for the carburization step was the same for both gear sets since they were carburized in the same batch (cf. Figure 2). Based on the differences between predicted stress states and their distributions (cf. Figure 3), a decision was made that this difference in grinding depth was acceptable and would not bias the fatigue data.

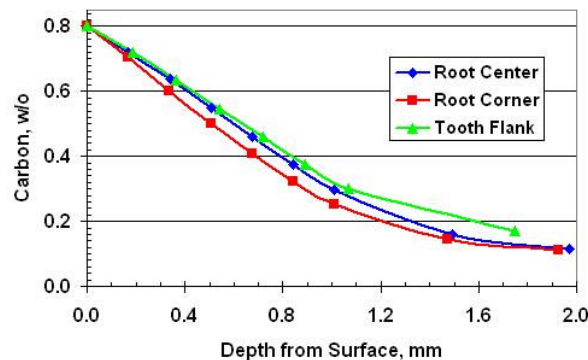


Figure 2: Predicted Local Carbon Profiles

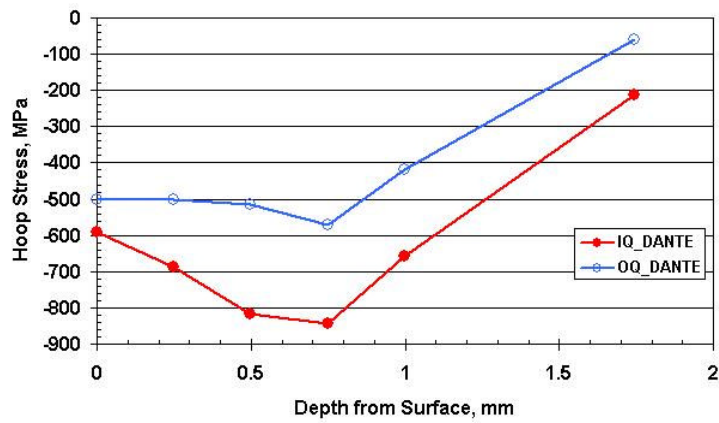


Figure 3: Circumferential (Hoop) Stress Predictions for Conventional Oil Quenched Gears and Intensively Quenched Gears

### 2.3 Comparison of Microstructures and Residual Stress

The microstructure and hardness values of the two gear populations were characterized. The microstructures for both quenching methods were tempered martensite (cf. Figures 4 and 5). The respective figures show the root – tooth fillet location and the carburized layer is evident (cf. Figure 4 and 5). The measured hardness of the intensively quenched gears was slightly higher than that of the oil quenched gears in the carburized case, but the core hardnesses were essentially the same (cf. Figure 6). These micrographs and microhardness measurements were made after finish grinding, and that is the reason for the somewhat lower than expected values for this carburizing schedule; values  $\geq Rc\ 60$  were measured on witness bars.

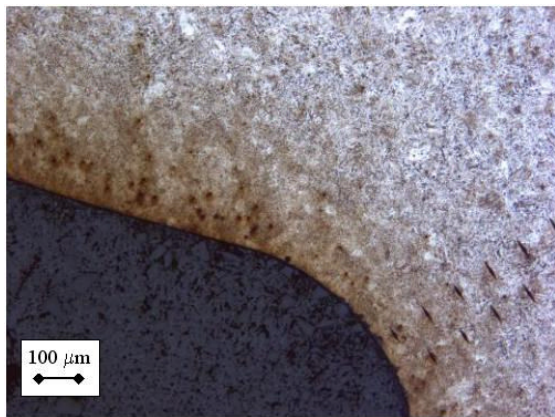


Figure 4: Microstructure of baseline gear.

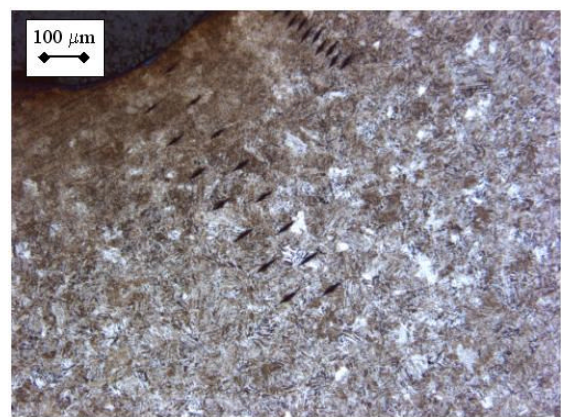


Figure 5: Microstructure of IQ gear.

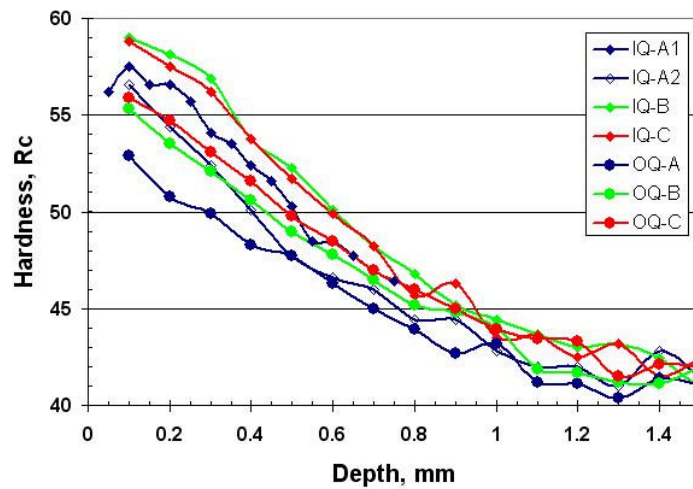


Figure 6: Microhardness vs. depth for the baseline (OQ) and intensively quenched (IQ) gears.

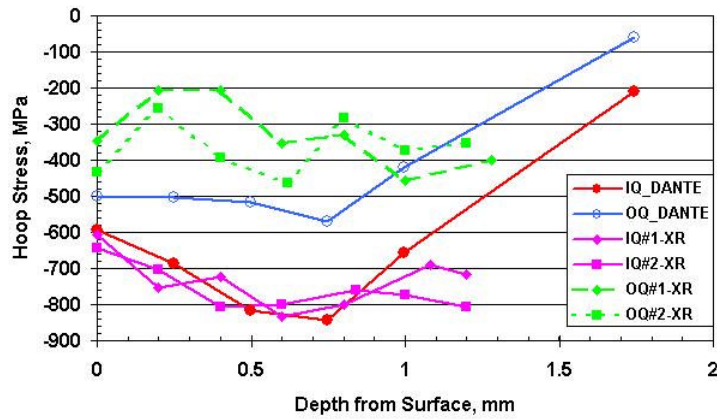


Figure 7: Circumferential (Hoop) stress vs. depth from the center of the root as determined from X-RAY diffraction measurements and as predicted by heat treat simulations.

X-RAY diffraction was performed on a baseline (OQ) gear and an intensively quenched (IQ) gear to compare residual stress values. Stress values as functions of depth for the stresses calculated from X-RAY diffraction measurements and by computer simulations showed that the intensive quenching process produced deeper compressive surface stress in the tooth root (cf. Figure 7). The minimum principal stress profile for the root fillet was predicted to be more compressive for both sets of gears, but with the difference between quench methods being even greater than at the root center. On the tooth face at approximately the pitch diameter, the two gears were found to have similar residual stress values by both the computer simulations and the X-RAY diffraction calculations.

## 2.4 Single Tooth Bending Fatigue Tests

The fixture used for tooth bending fatigue tests loaded two teeth simultaneously (cf. Figure 8). The ratio of minimum to maximum load was fixed at 1:10 so that one root fillet of each contacted tooth was always loaded in tension. The cycle frequency was 40 Hz, and the machine shut-off automatically when excessive ram displacement occurred. Runout was defined as  $10^7$  cycles without failure. The upper and lower anvils were shaped such that no teeth needed to be removed for load application. The location of the applied load was determined to simulate the point of first contact with a mating gear which would correspond to single tooth support and maximum stress in the gear root fillet. This is the typical failure location due to bending fatigue.

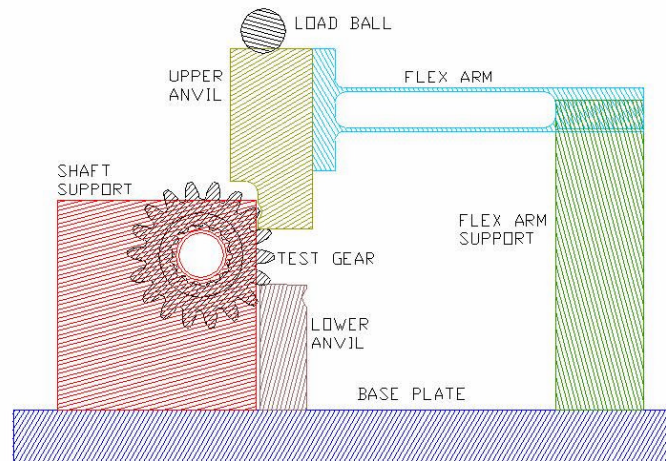


Figure 8: Schematic of single tooth bend test fixture at Gear Research Institute.

Qualitatively, the intensively quenched gears had higher fatigue life than the conventionally processed gears (cf. Figure 9). The number of runout data points ( $10^7$  cycles) are indicated along the runout limit line, with each runout case producing 2 data points since the teeth were tested

two at a time. A failure produced only one data point, that for the cracked tooth root. Statistical analysis of the fatigue data is yet to be done to quantify the difference between the two gear sets. Several failures occurred away from the root, and these are indicated in the plotted data (cf. Figure 9). The reasons for these abnormal failures has not yet been fully investigated. A preliminary observation using SEM has revealed sub-surface inclusions of sizes that should not be present in VIM-VAR steel.

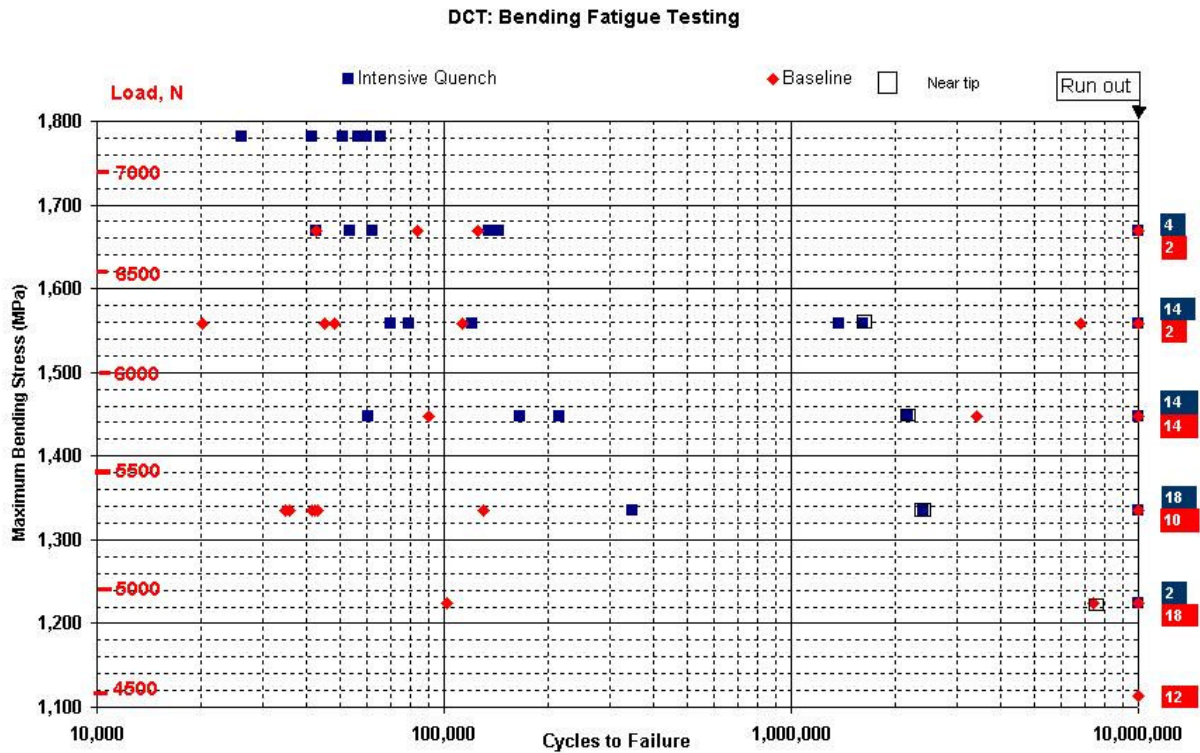


Figure 9: Single tooth bend fatigue data.

A typical fatigue failure originated at the outer surface of the root fillet and propagated inward (cf. Figure 10). The cracks examined thus far spanned the face of the fillet. Work is on-going to examine the fracture surfaces in detail.



Figure 10: Typical fatigue crack generated by cyclic tooth bending.

### 3 Discussion of Experimental and Simulation Results

The results from these single tooth bend tests show that higher surface compressive stress improves fatigue life, and that intensive quenching can produce higher compression than conventional oil quenching. These findings are in agreement with the results previously reported

for three point bend tests for this steel that were carburized and hardened using the schedules listed in Table 2 [Freborg, 2005]. Deeper surface compressive stress produced higher fatigue strength for parts having similar microstructures and hardness levels.

### 3.1 Martensite Formation & Evolution of Stress

The computer simulations can be used to determine the reasons for the differences in residual stress and dimensional change in these gears that end up with similar microstructures and hardness. The underlying reason for these differences between the two quench processes is the difference in the evolution of metallurgical phases caused by the differences in temperature histories during quenching. The heat treat simulations showed a significant difference in the timing of austenite transformation to martensite at specific locations in the gear. Figures are presented for martensite traces and minimum principal stress as a function of depth from the surface of the root center, and the keys to deciphering the step in the heat treat process are listed in Table 3.

Baseline Oil Quenching Process	Intensive Quenching Process
<b>A-T</b> : Austenitize & Transfer to Quench	<b>A-T</b> : Austenitize & Transfer to Quench
<b>OQ</b> : Oil Quench	<b>IQ</b> : Intensive Quench
<b>AC</b> : Cool to Room Temperature	
<b>DF</b> : Deep Freeze	<b>DF</b> : Deep Freeze
<b>RT</b> : Raise to Room Temperature	<b>RT</b> : Raise to Room Temperature
<b>Temper</b> : at Tempering Temperature	<b>Temper</b> : at Tempering Temperature
<b>Final</b> : at Room Temperature after Tempering	<b>Final</b> : at Room Temperature after Tempering

Table 3: Legend key for Figures 11 through 14.

For oil quenching, martensite formation started at roughly the case-core interface and transformation of the high carbon case to martensite occurred after significant martensite had developed internally (cf. Figure 11). In fact, much of the case transformed during the cooling period after oil quenching. This is in agreement with heat treating experience. Due to a sub-ambient martensite finish temperature in the high carbon surface, the level of retained austenite was high after quenching and cooling, and this necessitated cooling in liquid nitrogen. During the cryogenic step, the fraction of martensite in the case rose (cf. DF in Figure 11). Tempering converted the quenched martensite to tempered martensite and a corresponding minor increase in martensite content (cf. Figure 11).

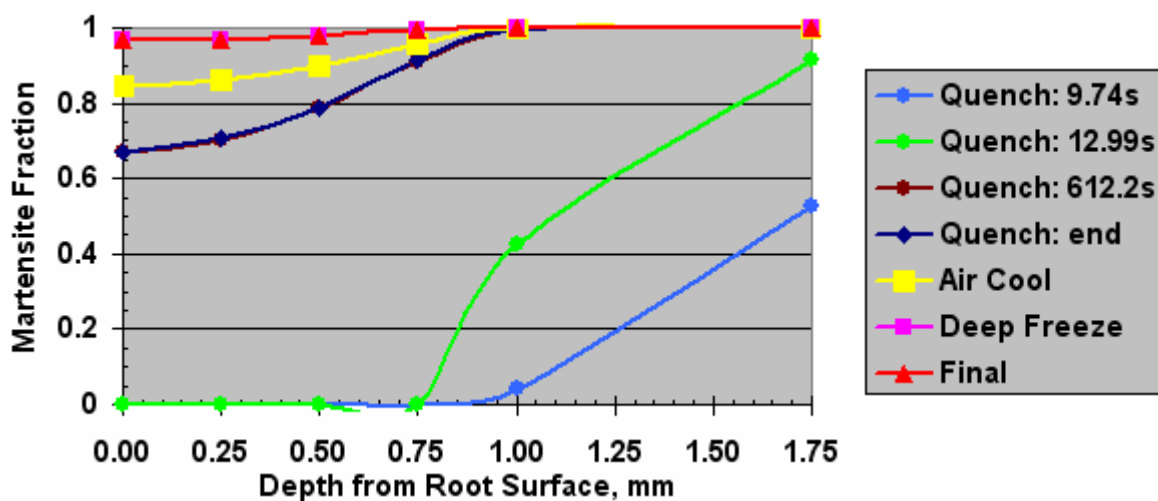


Figure 11: Martensite fraction vs. depth at the root center at the indicated baseline heat treat step.

The corresponding evolution of residual stress, as depicted by minimum principal stress changes with temperature and the local martensite volume fraction (cf. Figure 12). After austenitization

and transfer to the quench station, a small temperature gradient has developed and a small internal stress is evident (cf. A-T in Figure 12). After oil quenching, compressive stresses have developed, but the surface stress is less compressive due to lower martensite content (cf. OQ in Figures 11 and 12). Cooling to room temperature leads to further martensite formation in the case and deepening compression (cf. AC in Figures 11 and 12). The cryogenic treatment significantly increases compression by transforming near-surface austenite to martensite (cf. DF in Figures 11 and 12). The temperature rise to room temperature does not change the martensite content, but it does slightly decrease compression (cf. RT in Figures 11 and 12). The level of compression decreases somewhat during tempering (cf. Temper in Figure 12), and the final surface compression is predicted to be about -600 MPa upon cooling to room temperature (cf. Final in Figure 12).

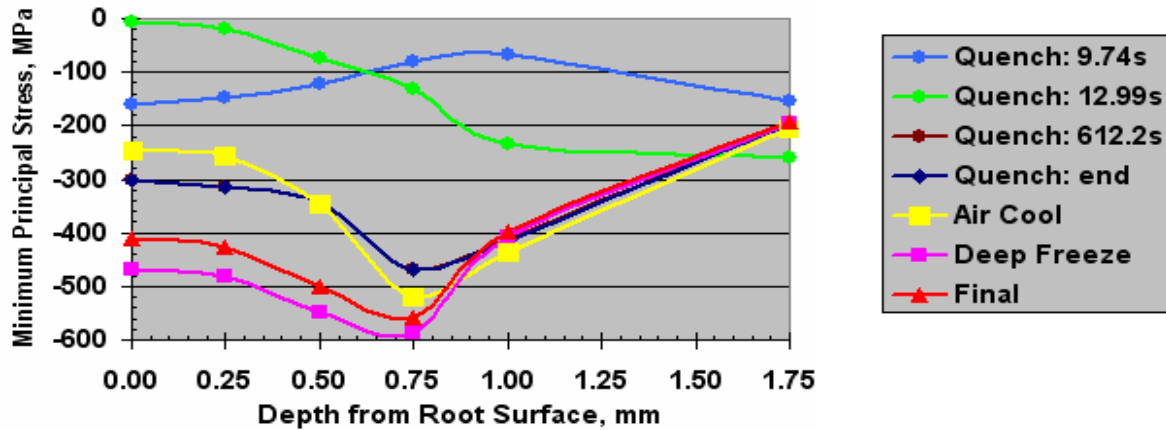


Figure 12: Minimum principal stress vs. depth at the root center at the indicated baseline heat treat step.

For intensive quenching, the severe cooling rate initiated austenite decomposition first in the high carbon case and then in the core of the gear. At the end of intensive quenching, the martensite content was predicted to be similar to that of oil quenching and air cooling (cf. IQ in Figure 13 and Air Cool in Figure 11). However, the timing differences in martensite formation resulted in a significant difference in the development of internal stress during quenching (cf. IQ in Figure 14 and AC in Figure 12). This significant difference in residual stress was maintained during the deep freeze and tempering steps so that the final residual stress state of the intensively quenched gear was more compressive than that of the baseline processed gear (cf. Final in Figures 12 and 14).

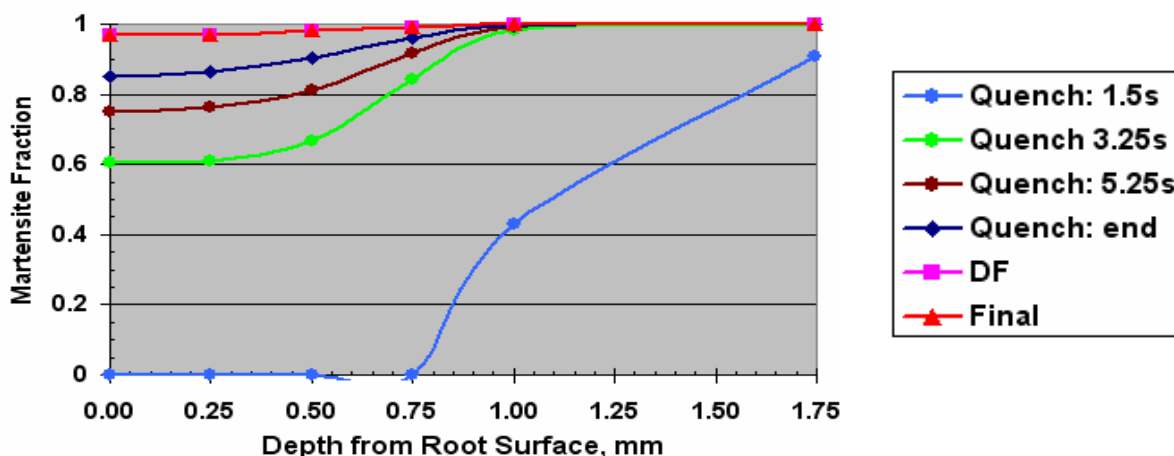


Figure 13: Martensite fraction vs. depth at the root center at the indicated IQ heat treat step.

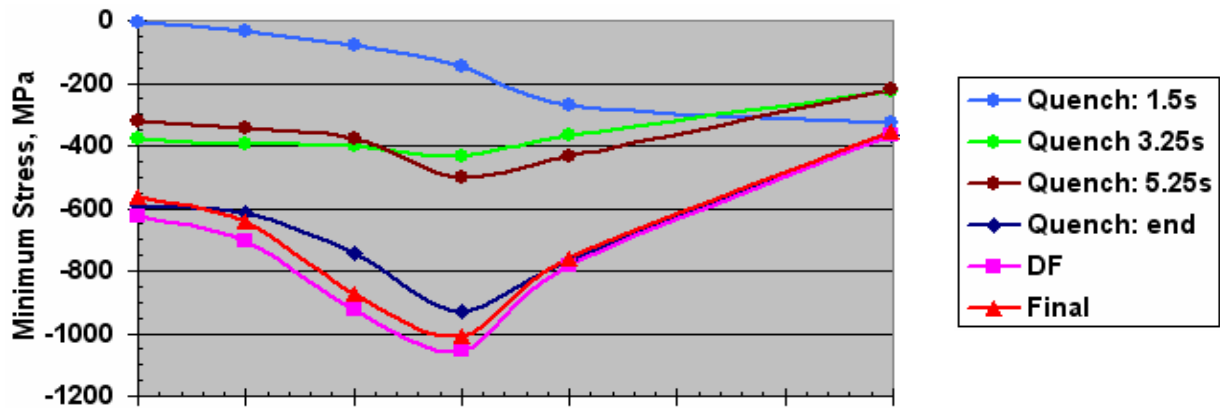


Figure 14: Minimum principal stress vs. depth at the root center at the indicated IQ heat treat step.

### 3.2 Stress State During Single Tooth Bend Testing

Computer simulation can also be used to study the change in stress state at the tooth root during fatigue testing. The maximum stress under load that is used to plot the fatigue data (cf. Figure 9) is calculated using an AGMA equation. [Dudley, 1984] This calculation computes the root stress at maximum load point, but it totally ignores the presence of the beneficial residual surface compression. The calculated values either exceed or are a significant fraction of the local yield strength, and this is not reasonable for a service environment that is limited by fatigue strength. If the residual compression from either oil quenching or from intensive quenching were not present, these gears would fail by simple overload, and not by fatigue. Finite element analysis provides a much truer estimate of the operating environment because the resultant stress state from heat treatment can be carried forward into the cyclic loading calculations (cf. Table 4). The benefit of residual surface compression in applications limited by fatigue strength is the reduction of tensile stress in the critically loaded regions of the part - the gear root fillet in this case. Both the baseline carburizing and quench hardening process and the intensive quenching process show marked lowering of maximum stress in comparison to an initially stress free condition (cf. Table 4). Furthermore, the deeper compression induced by intensive quenching results in a further reduction of maximum stress in comparison to the baseline oil quenching process.

Applied Load N	Maximum Stress by Lewis Eqn. [Dudley, 1984] MPa	Maximum Stress by AGMA Eqn. [Dudley, 1984] MPa	Maximum Stress by Finite Element Method MPa
6227.5	1346	1558	1600 : No Residual Stress
			1021 : OQ Residual Stress
			821 : IQ Residual Stress

Table 4: Maximum Stress in the Gear Root Calculated by AGMA and Finite Element Methods

## 4 Summary

The major findings of this study include:

- Intensive quenching can produce higher compressive surface stress than conventional oil quenching;
- Higher surface compressive stress improves gear tooth bending fatigue strength;
- Computer simulation can accurately predict the final residual stress state and the dimensional changes due to heat treatment;

- Computer simulation provides a tool to investigate the metallurgical events that occur during heat treatment such that the origins of the final stress state, distortion and metallurgical phases can be better understood; and
- Gear performance predictions should include the effect of residual stress because without it, many critically loaded gears would fail prematurely, not by fatigue but by simple overload.

Much more work remains to be done to continue to improve the fatigue life of critically loaded parts such as gears, bearings and shafts by heat treatment and other processes such as shot peening, surface burnishing and laser shockpeening. Some immediate questions relate to the effect of the thickness or depth of the compressive layer in addition to the magnitude of compression, and the interaction between these processes.

### **Acknowledgement**

This work was funded by the US Army AATD through SBIR Contract #W011W6-05-C-0017. The authors would like to thank B. Smith and E. Ames of AATD, J. Powell and M. Aronov of IQ Technologies, Inc., B. Hansen of Sikorsky Aircraft Corporation, S. Rao of the Gear Research Institute, D. Schwam and J. Wallace of Case Western Reserve University.

### **References**

- Dudley, Darle W., Handbook of Practical Gear Design, McGraw-Hill Book Company, New York, 1984.
- Freborg, Andrew, et al., "Bending Fatigue Strength Improvement of Carburized Aerospace Gears", Proceedings of the 23<sup>rd</sup> ASM HTS Conference, Sept. 25-28, 2005, pp 186-195.